Research Square

Preprints are preliminary reports that have not undergone peer review.
They should not be considered conclusive, used to inform clinical practice,
or referenced by the media as validated information.

The C-terminal LytR_C domain of essential LcpA contributes to cell envelope homeostasis and intracellular persistence in Mycolicibacterium smegmatis

Abhipsa Sahu
International Centre for Genetic Engineering and Biotechnology (Regional Research Centre)
Lijun Zhang
International Centre for Genetic Engineering and Biotechnology (Regional Research Centre)
Boris Tefsen
Utrecht University
David Ruiz-Carrillo
European Molecular Biology Laboratory
Jian-Mei Li
Nanjing Normal University
Yili Yang
yili.yang@icgeb.cn

International Centre for Genetic Engineering and Biotechnology (Regional Research Centre)

Research Article

Keywords: LCP protein, LytR_C domain, Mycolicibacterium smegmatis, cell wall integrity, peptidoglycan, arabinogalactan, anti-tuberculosis drugs, drug target

Posted Date: November 25th, 2026

DOI: https://doi.org/10.21203/rs.3.rs-11113139/v1

License: This work is licensed under a Creative Commons Attribution 4.0 International License.
Read Full License

Additional Declarations: No competing interests reported.

The C-terminal LytR_C domain of essential LcpA contributes to cell envelope homeostasis and intracellular persistence in *Mycolicibacterium smegmatis*

Abhipsa Sahu[1,4] $$, Lijun Zhang[1], Boris Tefsen[2], David Ruiz-Carrillo[3], Jian-Mei Li[4] and Yili Yang[1] $

[1] International Centre for Genetic Engineering and Biotechnology, Taizhou, Jiangsu, China

[2] Department of Molecular Microbiology, Utrecht University, Padualaan 8, Utrecht, Netherlands

[3] European Molecular Biology Laboratory, Notkestraße 85, Hamburg, Germany

[4]School of Food Science and Pharmaceutical Engineering, Nanjing Normal University, Nanjing, China

Running head: Role of LcpA-LytR_C domain in *Mycolicibacterium smegmatis*

$ Corresponding author: Yili Yang, yili.yang@icgeb.cn

$$ Co-corresponding author: Abhipsa Sahu, sahu.abhipsa@gmail.com

Conflict of interest: The authors declare that they have no conflicts of interest with the contents of this article.

ABSTRACT

Background: Tuberculosis (TB) remains the leading cause of mortality from a single infectious agent, and the prevalence of multidrug-resistant *Mycobacterium tuberculosis* (*Mtb*) strains underscores the urgency to identify novel therapeutic targets. The LytR-CpsA-Psr (LCP) family catalyzes the covalent ligation of arabinogalactan (AG) to peptidoglycan (PG), an essential step in mycobacterial cell wall assembly. While the catalytic LCP domain is well characterized, role of the C-terminal LytR_C domain remains elusive. Here, we investigated whether LytR_C is required for LcpA catalysis and how it contributes to envelope integrity, antibiotic susceptibility and intracellular persistence in *Mycolicibacterium smegmatis* (*Msmeg*).

Results: Recombinant LcpA lacking the transmembrane helix and LytR_C domain retained LcpA phosphotransferase activity, comparable to the LytR_C-containing soluble enzyme from both *Mtb* and *Msmeg*. In contrast, the chromosomal deletion of LytR_C from *lcpA* exhibited severely attenuated growth, a 1.6-fold prolonged doubling time, and profound morphological defects including pole-to-pole filamentation and failed septation. The mutant showed defective biofilm formation, increased sensitivity to Triton X-100 and lysozyme, and increased permeability to Nile Red, consistent with exposed AG and PG in the cell wall matrix. Consequently, the mutant demonstrated hypersensitivity to first-line anti-TB agents, and was rapidly cleared from THP-1-derived macrophages, with intracellular survival dropping to near-undetectable levels by 72 hours.

Conclusions: The LytR_C domain is dispensable for *in vitro* LcpA ligase activity but is indispensable for cell envelope architecture, cytokinetic fidelity, tolerance to cell-wall-targeting drugs and intracellular persistence. This functional dichotomy identifies the LytR_C domain as a compelling candidate for future validation as an adjunctive anti-TB therapeutic target that

compromises mycobacterial cell wall integrity, while circumventing competition with endogenous substrates at the catalytic active site.

KEYWORDS

LCP protein; LytR_C domain; *Mycolicibacterium smegmatis*; cell wall integrity; peptidoglycan; arabinogalactan; anti-tuberculosis drugs; drug target

BACKGROUND

Tuberculosis (TB) caused by *Mycobacterium tuberculosis* (*Mtb*) is one of the most lethal global public health threats, one of the major contributors to infectious disease-related mortality worldwide, together with HIV/AIDS [1, 2]. The prevalence of multidrug-resistant and extensively drug-resistant strains of *Mtb* further complicates TB control and raises concerns about the possible obsolescence of current anti-TB pharmacotherapies [1, 2]. This alarming trajectory accentuates the critical need to identify new pharmacological targets to help develop novel and more effective treatment strategies. Current frontline anti-TB therapies predominantly focus on inhibiting cell wall synthesis, thereby disrupting a fundamental structural component necessary for bacterial viability and virulence [3, 4].

Bacteria must constantly synthesize and modulate their cell envelopes to sustain growth and withstand environmental stresses. The primary supporting layer of the mycobacterial cell envelope is peptidoglycan (PG), a single macromolecular heteropolysaccharide composed of glycan strands cross-linked by short peptides [5]. Insufficient cleavage of PG hinders cellular proliferation, whereas excessive hydrolysis renders cells susceptible to osmotic lysis [6]. Consequently, the hydrolases responsible for PG turnover require stringent spatiotemporal regulation. In Gram-positive bacteria,

glycopolymers covalently linked to PG serve as candidate signaling molecules that report the status of PG synthesis to membrane-associated protein complexes [7], as their lipid-linked precursors are translocated from the inner to the outer leaflet of the cytoplasmic membrane and subsequently transferred to nascent PG by membrane-anchored LytR-CpsA-Psr (LCP) family enzymes [8].

The LCP enzymes are widely conserved across both Gram-positive and Gram-negative bacterial phyla, with most species encoding multiple paralogs [9]. *Mtb* and its non-pathogenic surrogate model *Mycobacterium smegmatis* (*Msmeg*) each encode four LCP proteins: LcpA (Rv3267/MSMEG_1824), LcpB (Rv3484/MSMEG_0107), and LcpC (Rv0822c/MSMEG_5775) and LcpD (Rv3840/MSMEG_6421). Members of the LCP family function as glycopolymer ligases, facilitating the covalent attachment of different glycopolymers to PG [10]. In Gram-positive organisms, LCP enzymes facilitate the transfer of a broad variety of undecaprenyl-phosphate (C_{55}-P)-linked polymers onto nascent PG [11-17]. Synthetic lethality and biochemical reconstitution investigations have confirmed LcpA as the primary enzyme responsible for AG-PG ligation in mycobacteria [14], whilst LcpB and LcpC offer supportive redundancy and LcpD is barely engaged in this process [18]. Despite substantial progress in defining the catalytic LCP domain, the functional relevance of the accessory C-terminal LytR_C domain in actinobacterial LcpA orthologs has remained inexplicable. Notably, both LCP and LytR_C domains are found in bacterial genomes either separately or together, indicating distinct yet potentially interdependent functions [16, 19-21].

Here, we demonstrate that deletion of the LytR_C domain from the essential LcpA in *Msmeg* leads to phenotypic manifestations consistent with compromised PG integrity and envelope homeostasis. We demonstrate that the LytR_C domain is structurally and functionally independent from the crucial catalytic activity of LcpA, and instead plays a critical role in maintaining cell envelope architecture. However, this C-terminal accessory domain is esssential for a robust cell envelope.

Consequently, these findings propose a paradigm in which the LytR_C domain functions as a structural scaffold that coordinates cell wall assembly, thereby identifying a novel target for therapeutic intervention against mycobacterial infections.

MATERIALS AND METHODS

Bacterial strains, plasmids and culture conditions

Msmeg strain mc^{2}155 (ATCC 607) was obtained from China General Microbiological Culture Collection Center (CGMCC). *Mtb* genomic DNA was previously isolated in our lab [18]. All bacterial strains and plasmids used in this study are listed in Table S1. Nucleotide sequences of the *Msmeg* mc²155 genome (GenBank accession number CP000480.1) were used for the design of all recombinant and knockout plasmid constructs. *E. coli* strains were cultivated in Luria-Bertani (LB) broth or on LB agar at 37°C with shaking at 200 rpm, supplemented with antibiotics (100 μg mL^{-1}) where appropriate. *Msmeg* WT and *lcpΔlytR_C* deletion mutant strains were grown in Middlebrook 7H9 broth (Difco) supplemented with 10% ADS [18]. Seed cultures were grown overnight at 37°C with shaking at 200 rpm. Overnight experimental cultures were inoculated at a 1:100 dilution into fresh 7H9 medium supplemented with Tween-80. All the inhibitors in this study were purchased from MedChemExpress (MCE, China), unless indicated.

Construction of the lcpAΔlytR_C mutant strain

The allelic replacement strategy for gene deletion in *Msmeg* was adapted from the Niederweis group [22] and previously established in our laboratory for generating *lcp* deletion mutants [18]. The

unmarked *lcpA*Δ*lytR_C* deletion mutant was verified by PCR using knockout confirmation primers (Table S2) and by RT-qPCR.

RNA extraction and RT-qPCR

Bacterial cultures were grown at 37°C with shaking at 200 rpm, and the OD_{600} was monitored using a UV-Vis spectrophotometer. Cells were harvested by centrifugation at 11,000 × *g* for 2 min, resuspended in 100 µL TE buffer (10 mM Tris-HCl, pH 8.0, 0.1 mM EDTA), and treated with lysozyme (2 mg mL^{-1} final concentration) to disrupt the mycobacterial cell wall. Total RNA was extracted using the EasyPure® RNA kit (Transgen Biotech, China) according to the manufacturer's instructions, followed by reverse transcription to cDNA using the GoScript™ Reverse Transcription System (Promega). Gene expression was quantified by qPCR (Applied Biosystems® 7500, Thermo Fisher Scientific) using GoTaq® qPCR Master Mix (Promega) and gene-specific primers (Table S2), with *rpoD* (*sigA*) serving as the reference gene. Relative expression levels were calculated using the $2^{-\Delta\Delta Ct}$ method.

Growth kinetics and doubling time determination

Growth of WT and *lcpA*Δ*lytR_C* deletion strain was monitored in polystyrene 96-well plates (Corning) using a microplate reader (GloMax® Discover, Promega). Overnight cultures were adjusted to an OD_{600} of 0.5 and diluted 1:20 into fresh medium. A total volume of 200 µL per strain was plated in triplicate and incubated at 37°C for 60 h, with OD_{600} readings recorded every 8 h. Doubling time was calculated using the formula: Doubling time = [duration × log(2)] / [log(final concentration) − log(initial concentration)] [23].

Scanning electron microscopy (SEM)

For SEM, bacterial cells were fixed with 2.5% (v/v) glutaraldehyde (Macklin) in phosphate-buffered saline (PBS) and processed by Yuan Test Company (Qingdao, China). Sample preparation is an adaptation from a previous study [16]. Briefly, fixed cells were washed in PBS for 15–30 min and dehydrated through an ascending acetone series (30%, 50%, 70%, 90%, and 100%), with the final 100% step repeated three times (15–20 min per step). Samples were critical-point dried in liquid CO_2, sputter-coated with a 10-nm gold/palladium layer, and analyzed using an environmental scanning electron microscope (ESEM XL 30 FEG, FEI/Philips, Eindhoven, Netherlands) in high vacuum at 10 kV acceleration voltage.

Colony morphology and Congo Red binding assays

Colony morphologies of WT and the mutant strain were assessed on 7H10 agar supplemented with 10% ADS, , 0.05% Tween-80 and 100 μg mL^{-1} [1] Congo Red [24]. Overnight cultures were adjusted to an OD_{600} of 0.5, and 5 μL aliquots were spotted in triplicate onto agar plates. Plates were incubated at 37°C for 2 days in sealed plastic bags. Colonies were inspected visually, and colony diameter was determined by averaging two perpendicular measurements per colony.

Biofilm formation and quantification

Pellicle formation at the air-liquid interface was evaluated using a static-culture assay adapted from established mycobacterial biofilm protocols [25, 26], with modifications. Overnight cultures were standardized to an OD_{600} of 0.5 and inoculated at a 1:100 dilution into 20 mL 7H9+10% ADS medium. To promote cell–cell aggregation and pellicle maturation, Tween-80 was deliberately

154 excluded from the medium, as surfactants disrupt the hydrophobic interactions required for
155 mycobacterial aggregation at the air–liquid interface [27]. Cultures were incubated under stationary
156 conditions at 37°C for 4–5 days to allow robust pellicle development. Biofilm formation was
157 assessed by crystal violet staining as described previously [25], with modifications. Overnight
158 cultures were washed with 7H9+10% ADS medium, diluted to a final OD_{600} of 0.05 in 7H9+10%
159 ADS medium, and 200 µL aliquots were dispensed into each well of a 96-well polystyrene plate
160 (Corning). Plates were incubated at 37°C for 5 days. After incubation, culture supernatants were
161 discarded, and wells were washed 2–3 times with distilled water. Adherent biofilms were stained
162 with 1% crystal violet for 1 h at room temperature, washed 3–4 times with water, and air-dried.
163 Bound dye was solubilized in 300 µL of 80% (v/v) ethanol, and absorbance at 550 nm was
164 measured using a microplate reader (GloMax® Discover, Promega).
165
166 ***Triton X-100 and Lysozyme susceptibility assays***
167 Overnight cultures were subcultured at 37°C. Cells were harvested during mid-log phase,
168 normalized to an OD_{600} of 0.5 in PBS, and treated with either 0.01% Triton X-100 (Thermo Fisher
169 Scientific) for 2 h or 0.125 mg/mL lysozyme (Sigma-Aldrich) for 24 h at 37°C. Following
170 treatment, serial 10-fold dilutions were prepared and plated onto 7H10 agar. Plates were incubated
171 at 37°C for 2–3 days until colonies were visible. Survival was quantified by comparing CFUs from
172 treated versus untreated cells.
173
174 ***Cell membrane permeability assay***
175 Cell envelope permeability was assessed by Nile Red dye influx as described previously [28], with
176 modifications. Overnight cultures were diluted to an OD_{600} of 0.05 in 7H9 medium with ADS

supplement and incubated until OD_{600} = 0.8 at 37°C with shaking at 220 rpm. Cells were pelleted by centrifugation at 12,000 rpm for 2 min, washed twice with PBS containing 0.05% Tween-80, and resuspended in 1 mL 7H9 medium. Aliquots (100 µL) were transferred in triplicate to a 96-well black fluoroplate (Corning®, USA), and Nile Red was added to a final concentration of 20 µM. Fluorescence was measured continuously for 48 h with excitation at 540 nm and emission at 630 nm. All data were normalized to the T = 0 reading for each well.

Direct ELISA for arabinogalactan detection

Direct ELISA was performed as described previously [18]. Briefly, overnight cultures of the *Msmeg* strains were washed twice with PBS and resuspended to a final concentration of 1.5×10^8 cells per well in 50 mM carbonate coating buffer. 150 µL were added to each well of NUNC™ MaxiSorp™ 96-well plates and incubated overnight at 4°C. Plates were air dried, washed twice with PBS containing 0.05% Tween-20 (PBST), and blocked with 1% bovine serum albumin (BSA) in PBST for 1 h at room temperature. Wells were incubated with 150 µL of horseradish peroxidase (HRP)-conjugated EB-A2 monoclonal antibody (0.2 mg mL^{-1} in PBST) overnight at 4°C. After washing twice with PBST, 200 µL of TMB substrate solution was added to each well and incubated for 30 min at room temperature with gentle shaking. The reaction was terminated by addition of 50 µL of 0.8 M H_2SO_4, and absorbance was measured at 450 nm using GloMax® Discover microplate reader (Promega).

Indirect ELISA for peptidoglycan detection

Mouse anti-PG monoclonal antibody clone 3F6B3 (10H6) (Bio-Rad), which recognizes epitopes comprising separated glycan and/or amino acid residues within the three-dimensional structure of

bacterial PG, was used for PG detection. ELISA plates were prepared as described for AG detection. Goat anti-mouse secondary antibody (1:8,000 dilution) was used for detection, followed by TMB substrate development and absorbance measurement at 450 nm.

For ELISA detection from AG-PG extract of cell wall components, we followed the extraction protocol as described in our previous study [18].

Antibiotic susceptibility assays

MIC values were determined using the resazurin microtiter assay (REMA) as described previously [29] , with minor modifications. Briefly, overnight cultures were adjusted to an OD_{600} of 0.5 and diluted 1:1000. In a 96-well polystyrene plate (Corning), 50 µL of 7H9 medium supplemented with 10% ADS was added to all wells except the first row. Antibiotic stock solutions at double the required concentration were prepared, and 100 µL was added to the first row. Serial two-fold dilutions were performed by transferring 50 µL to 50 µL of medium in subsequent rows. The final row contained medium only (negative control). Then, 50 µL of diluted bacterial culture was added to each well to achieve the desired final antibiotic concentration. Plates were sealed in plastic bags and incubated at 37°C for 48 h, after which 30 µL of filter-sterilized 0.2 mg mL^{-1} resazurin dye was added to each well and incubated overnight at 37°C. The MIC was defined as the lowest antibiotic concentration at which resazurin color remained unchanged (indicating growth inhibition).

MIC spot assays were performed on Congo Red agar plates. Overnight cultures were adjusted to an OD_{600} of 0.5, diluted 1:1,000, treated with the indicated antibiotic concentrations, and 5 µL aliquots were spotted onto agar plates. Plates were incubated at 37°C for 2–3 days until colonies appeared.

223

224 ***Cloning, overexpression, and purification of recombinant LcpA variants***

225 Genomic DNA was extracted from *Msmeg* WT mc²155 and *Mtb* hospital strain using standard
226 protocols. Transmembrane spanning regions were predicted using the TMHMM server (Expasy).
227 The following constructs were generated: LcpAΔTM$_{Msmeg}$ (amino acids 25–493),
228 LcpAΔTMΔLytR_C$_{Msmeg}$ (amino acids 25–352), LcpAΔTM$_{Mtb}$ (amino acids 38–498), and
229 LcpAΔTMΔLytR_C$_{Mtb}$ (amino acids 38–364). All constructs were cloned into appropriate vectors
230 (Table S1) with an N-terminal hexahistidine (6×His) tag. Constructs were verified by colony PCR,
231 restriction digestion, and Sanger sequencing (Genewiz/Azenta Life Sciences, Suzhou, China).
232 For protein expression, recombinant plasmids were transformed into *E. coli* BL21 (DE3).
233 Individual colonies were inoculated into 500 mL LB broth supplemented with ampicillin (100 μg
234 mL^{-1}) and grown overnight. A 100-mL aliquot of overnight culture was used to inoculate 1 L of
235 fresh LB broth, which was grown to an OD_{600} of 0.6 at 37°C. Protein expression was induced with
236 0.2 mM isopropyl β-D-1-thiogalactopyranoside (IPTG). Cells were harvested and disrupted by
237 sonication on ice (amplitude 30%, pulse-on 5 s, pulse-off 10 s, total time 3 min; QSonica). Lysates
238 were centrifuged at 40,000 × *g* for 45 min at 4°C, and the supernatant was filtered through a 0.22-
239 μm membrane (Millipore). Filtered lysates were applied to Ni-NTA agarose beads (Bio-Rad)
240 equilibrated in lysis buffer. The column was washed three times with 10 mL lysis buffer, followed
241 by a final wash in lysis buffer containing 0.15 mM *n*-dodecyl β-D-maltoside (BBI Life Sciences)
242 to release endogenous lipids. Protein was eluted with elution buffer and concentrated using a 10-
243 kDa cutoff Amicon® Ultra-15 centrifugal filter (Millipore). Concentrated protein (5 mL) was
244 further purified by size-exclusion chromatography on a HiLoad™ 16/600 Superdex™ 200 pg
245 column (Cytiva) coupled to an ÄKTAprime plus FPLC system (GE Healthcare). Eluted fractions

were monitored at 280 nm and analyzed by SDS-PAGE. Fractions containing the target protein were pooled, concentrated, and stored at −80°C. GST- and/or His-tagged LcpAΔTM fusion proteins were used for all assays.

In vitro phosphotransferase (ADP-Glo™) assay

The *in vitro* phosphotransferase activity of LcpAΔTM and LcpAΔTMΔLytR_C variants from *Msmeg* and *Mtb* was measured using the ADP-Glo™ kinase assay (Promega) in Corning® 384-well white polystyrene microplates (Sigma-Aldrich). Each 5-µL reaction contained 5 µM purified recombinant protein, 1× kinase reaction buffer A (pH 7.5), 20 mM $MgCl_2$, 274 µM geranyl pyrophosphate (GPP), and 10 µM ATP. Reactions were incubated at 25°C for 1 h, terminated by addition of 5 µL ADP-Glo™ reagent, and incubated for an additional 40 min at 25°C. Then, 10 µL of kinase detection reagent was added, and plates were incubated for 30 min at 25°C. Luminescence was detected using GloMax® Discover microplate reader (Promega) with an integration time of 0.5–1 s. ATP levels, measured as relative light units (RLU), were converted to percentage ATP-to-ADP conversion using a standard curve.

Phylogenetic and sequence analysis

Phylogenetic analysis was performed using MEGA 11 [30]. Evolutionary relationships were inferred using the neighbor-joining method [31], and evolutionary distances were computed using the p-distance method (units: amino acid substitutions per site) [32]. Confidence limits were evaluated by bootstrapping with 10,000 replicates. Rate variation among sites was modeled with a gamma

distribution (shape parameter = 1). Multiple sequence alignments of LytR_C domains were generated using ClustalW with the PAM250 matrix and visualized using ESPript 3.0.

THP-1 cell culture, differentiation, and infection assays

THP-1 monocytes (ATCC TIB-202) were maintained in RPMI 1640 medium (Gibco, Thermo Fisher Scientific) supplemented with 10% heat-inactivated fetal bovine serum (FBS; Gibco) and 1% penicillin-streptomycin (Invitrogen) at 37°C in a humidified incubator with 5% CO_2. Differentiation into macrophage-like cells was achieved by exposure to 20 ng/mL phorbol 12-myristate 13-acetate (PMA; Sigma-Aldrich) for 24 h, with successful differentiation verified by adherence and morphological changes observed by phase-contrast microscopy.

For infection assays, differentiated THP-1 macrophages were seeded at appropriate densities and infected with *Msmeg* strains at a multiplicity of infection (MOI) of 5. Infected cells were incubated for 3 h at 37°C in 5% CO_2 to allow phagocytosis. Extracellular bacteria were eliminated by washing three times with 1× PBS, followed by addition of complete RPMI medium containing gentamicin (10 μg mL^{-1}). After three additional PBS washes, cells were maintained in fresh medium. At indicated time points (0, 8, 16, 24, 48, and 72 h), macrophage monolayers were washed with PBS and lysed with 0.1% Triton X-100 in 7H9 medium. Lysates were serially diluted and plated onto 7H10 agar. Following 2-3 days of incubation at 37°C, viable intracellular bacteria were enumerated as CFU. For drug treatment experiments, INH, EMB, or VAN was added to a final concentration of 10 μM 2 hours after the gentamicin kill step. Three independent experiments were conducted, each in duplicate.

Statistical analysis

All experimental data were analyzed using GraphPad Prism 10.0 software. Data distribution was assumed to be normal based on prior experimental validation, and experiments were repeated multiple times to ensure reproducibility. Statistical significance between groups was determined by one-way or two-way analysis of variance (ANOVA) with Dunnett's or Tukey's post-hoc test (as indicated in figure legends) at a 95% confidence level. A P value < 0.05 was considered statistically significant. Data are presented as mean ± standard deviation (SD) or median with interquartile range, representing the averages of technical replicates from the indicated number of independent biological experiments.

RESULTS

Evolutionary conservation and domain architecture of actinobacterial LytR_C-containing LCP proteins

The Msmeg mc2155 genome encodes four paralogous LCP proteins with different structural configurations [18]. The essential MSMEG_1824 (LcpA) has a brief cytoplasmic region at the N-terminus, a single transmembrane helix, the catalytic LCP domain and an uncharacterized C-terminal LytR_C domain conserved among closely related actinobacterial species (Fig 1A). The LytR_C domain exhibits comparable length across phylogenetically related species, suggesting functional constraint. Phylogenetic analysis of LytR_C domains from Lcp homologs revealed distinct clades for LcpA, LcpB (MSMEG_0107) and LcpC (MSMEG_5775) orthologs (Fig 1B). Interestingly, the LytR_C domains of LcpA and LcpB clustered within a larger clade, whereas the LytR_C domain of LcpC segregated outside this cluster, potentially reflecting functional divergence. Sequence alignment identified six fully conserved residues across all LytR_C-

containing Lcp proteins in the analyzed species (Fig 1C), indicating that these amino acids play a conserved and non-redundant role in cell wall assembly.

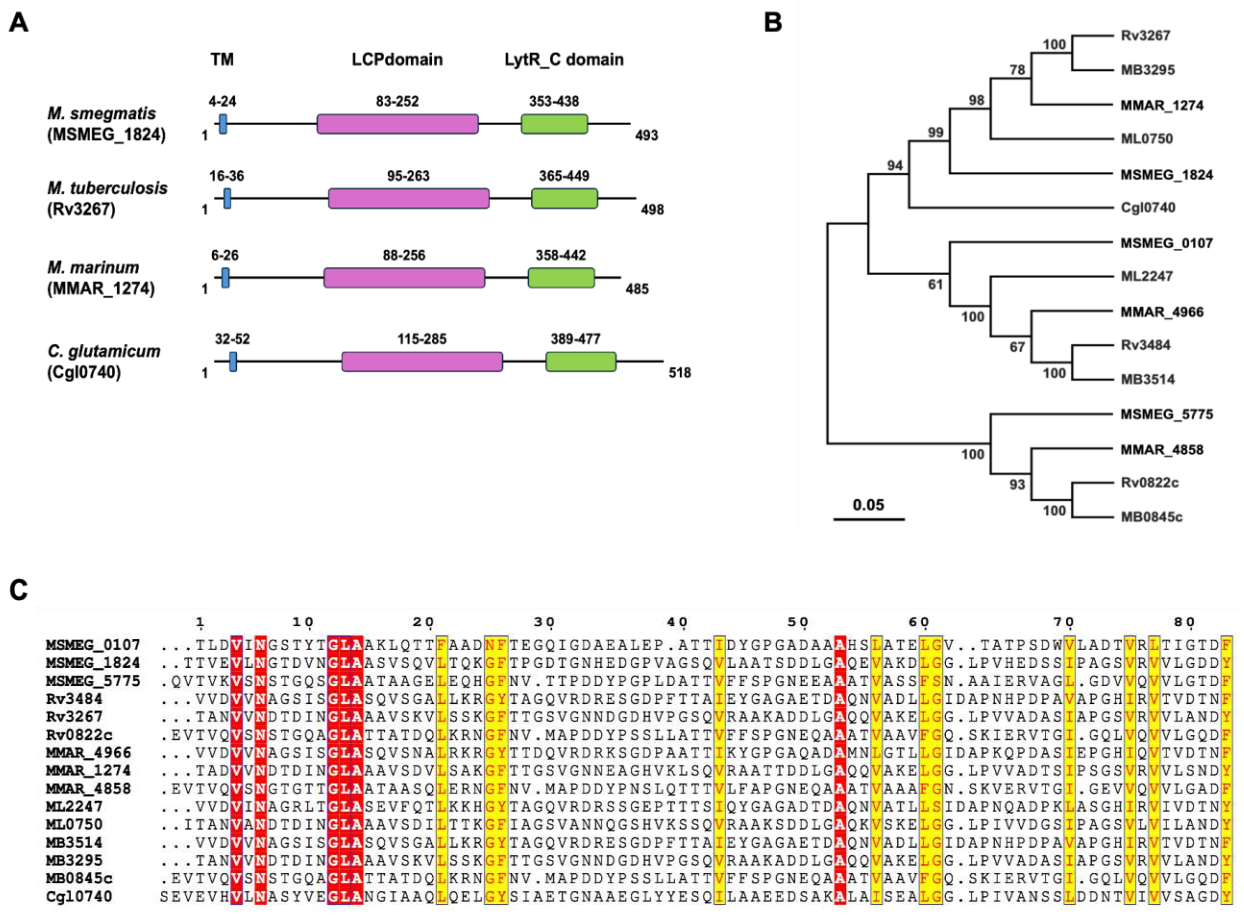

Fig 1. Overview of the LytR_C domain of LCP proteins. A. Domain organization of LcpA across actinobacteria. The three domains of the full-length LcpA protein from *Msmeg*, along with homologous proteins from closely related species, were systematically delineated to scale following the identification of their corresponding amino acid sequences in the UniProt database. **B.** Evolutionary relationships among taxa. The evolutionary lineage was deduced through the Neighbor-Joining approach [31]. The ideal tree displaying a total branch length of 2.779 is presented. The percentage of replicate trees in which the associated taxa clustered together in the bootstrap analysis (10,000 iterations) is indicated next to the branches [33]. The evolutionary distances were calculated using the p-distance method [32], expressed in terms of the number of amino acid differences per site. The analysis involved 15 amino acid sequences. A pairwise

deletion method was employed, which removed all ambiguous positions from each sequence pair, resulting in a final dataset with 89 positions. Evolutionary analyses were performed in MEGA11 [30, 34], utilizing a maximum of 7 parallel computing threads. **C.** Multiple sequence alignment of the LytR_C domain of LCP proteins across different actinobacterial species. The amino acid sequences are aligned employing ClustalW utilizing the PAM250 matrix and visualized using EsPRIPT 3.2 [35]. Amino acids that are completely conserved throughout the alignment are depicted in white against a red backdrop. Homologous amino acid residues are shown in red and enclosed within a yellow box.

The LytR_C domain is dispensable for in vitro phosphotransferase activity

To evaluate whether the C-terminal LytR_C domain contributes to the essential catalytic function of LcpA in covalently linking AG to PG [14], we purified recombinant soluble variants lacking the N-terminal transmembrane domain (ΔTM) and variants lacking both the transmembrane domain and the C-terminal LytR_C domain (ΔTMΔLytR_C) from both *Mtb* and *Msmeg*, and subjected them to an ADP-Glo™ kinase activity assay (Fig 2A). The specific ligase activity of LcpA$_{_Mtb}$ΔTM was approximately 0.52 μM min^{-1} $μM^{-1}$ enzyme, whereas the double-truncated variant LcpA$_{Mtb}$ΔTMΔLytR_C displayed a comparable activity of ~0.50 μM min^{-1} $μM^{-1}$ enzyme (Fig. 2A). Similarly, for the *Msmeg* ortholog, LcpA$_{Msmeg}$ΔTM and LcpA$_{Msmeg}$ΔTMΔLytR_C exhibited nearly identical specific activities of ~0.39 μM min^{-1} $μM^{-1}$ enzyme. Statistical analysis revealed no significant difference between the ΔTM and ΔTMΔLytR_C variants within either species (Fig. 2A). Notably, both *Mtb* variants showed significantly higher ligase activity than their *Msmeg* counterparts, consistent with previous observations [18]. These results demonstrate that the C-terminal LytR_C domain is dispensable for the *in vitro* phosphotransferase/ligase activity of

LcpA in both mycobacterial species, and that the catalytic core residing within the LCP domain is sufficient to sustain full enzymatic activity under the assay conditions tested.

Chromosomal deletion of the LytR_C domain attenuates growth and disrupts cellular morphogenesis

Having established the catalytic dispensability of the LytR_C domain, we next assessed whether chromosomal deletion of this domain elicited ligase-independent physiological alterations at the cell surface. Therefore, we generated an unmarked knockout mutant devoid of LytR_C domain in *lcpA* gene (*lcpAΔlytR_C*) in *Msmeg* via allelic replacement [18, 22] and confirmed the deletion by PCR and RT-qPCR (Fig 2B, i and ii). However, our attempt to generate a complement construct of the LcpA-LytR_C domain by replacing the endogenous *hsp*60 promoter of pSMT3 plasmid with *rfbD* (*MSMEG_1825*) that is upstream of *lcpA* (*MSMEG_1824*) and harbors the potential promoter region of *lcpA*, remained unsuccessful. This could be because LytR_C was expressed as an isolated plasmid-borne domain, thereby limiting the recreation of the native protein architecture in the complement construct. Compared to the wild-type (WT) mc²155 strain, the *lcpAΔlytR_C* mutant exhibited significantly attenuated growth, with a maximum 1.9-fold reduction in optical density at 48 h and a 1.2-fold increased doubling time (Fig 2C, i and ii).

To determine whether the growth defect reflected impaired cytokinesis, we performed scanning electron microscopy (SEM) on mid-log phase cultures. While the WT *Msmeg* displayed characteristic short, rod-shaped bacillary morphology with smooth surfaces and regular dimensions, the *lcpAΔlytR_C* mutant exhibited a pronounced filamentous phenotype, with cells appearing markedly elongated and irregular (Fig 2D, i). Quantification revealed that the median cell length of the WT strain was approximately 3 μm, consistent with established dimensions for

Msmeg mc²155 [36]. The mutant displayed a significantly increased median cell length of approximately 6.5–7 µm, representing an approximately 2-fold elongation relative to the WT (Fig 2D, ii). This filamentous morphology of the mutant is indicative of failed septation, a process that under WT conditions is intricately linked and coordinated predominantly from the poles [37, 38]. Expression of the LytR_C domain in trans significantly reduced the median cell length to approximately 4–5 µm relative to the *lcpAΔlytR_C* mutant, although cell lengths remained greater than those of the WT strain (Fig 2D, ii). This partial rescue supports a contribution of LytR_C to normal cell morphology.

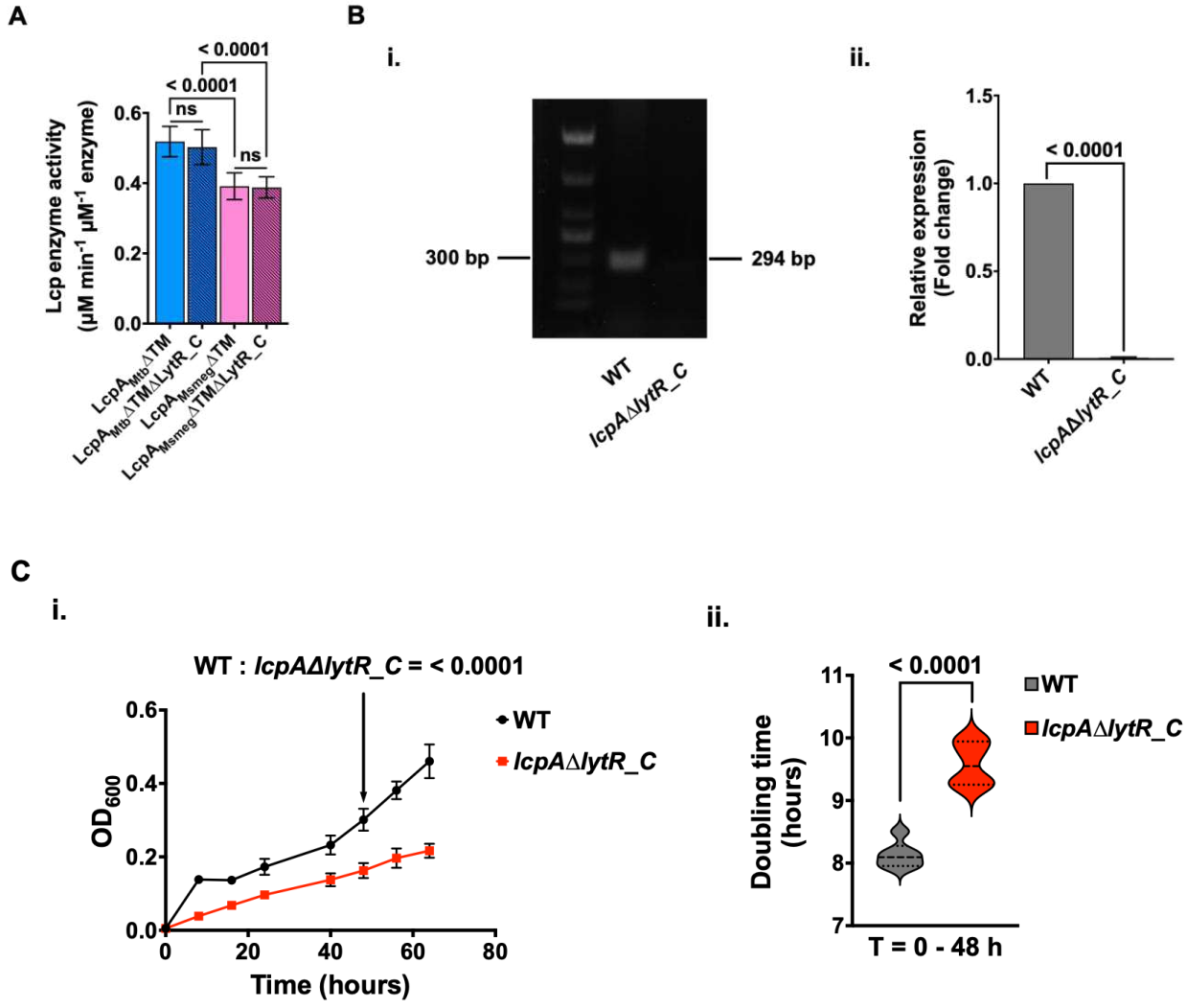

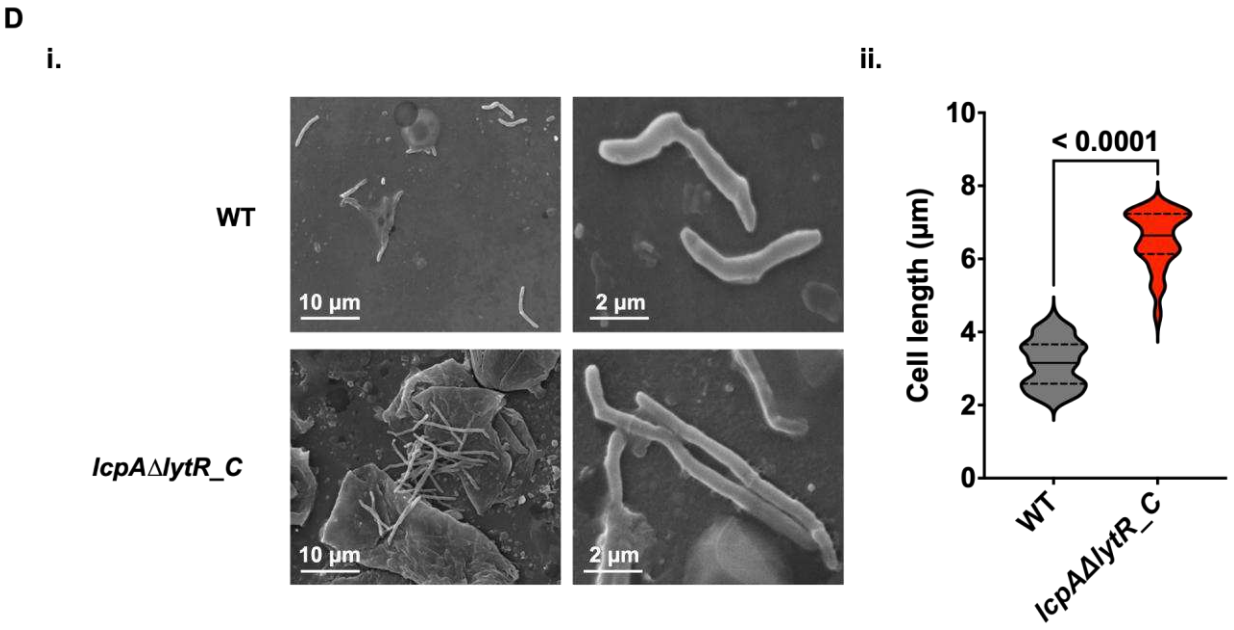

Fig 2. Alteration of replicative properties in the *lcpAΔlytR_C* mutant. A. *In vitro* catalysis. The phosphotransferase activity of *Mtb* and *Msmeg* LcpA homologs devoid of LytR_C domain was assessed through the ADP-Glo™ kinase assay, with GPP as the substrate. In this study, the total quantity of ADP produced during the phosphorylation process was quantified. The presented data is an average of four independent experiments each performed in duplicate, and the error bars represent ± SD between the experiments. Statistical significance was determined by ordinary one-way ANOVA with Tukey's post-hoc analysis (95% confidence level). **B.** Confirmation of *lcpAΔlytR_C* mutant. Agarose gel electrophoresis (i) and RT-qPCR (ii) showing confirmed LytR_C domain deletion of *lcpAΔlytR_C* mutant as compared to the WT strain. **C.** (i) Growth curve showing continuous growth over a 64-hour timeline. (ii) The doubling time was determined from the optical density curve at T = 0h - 48h range. Data presented is an average of three independent experiments in duplicate, with error bars indicating standard deviation. Ordinary one-way ANOVA with Dunnett's post-hoc analysis (95% confidence level) was used to determine statistical significance at T=48h. **D.** SEM analysis showing (i) cell morphology of *Msmeg* strains and (ii) Interleaved violin plot (Median-line, Quartile-dashed) showing quantification of the cell length from 50 individual cells

out of two independent experiments. Two-way ANOVA with Dunnett's multiple comparisons test (95% confidence level) was used to determine statistical significance.

Loss of the LytR_C domain compromises cell wall integrity and permeability

To investigate whether deletion of the LytR_C domain altered cell wall morphology, we cultivated strains on Congo red (CR) agar plates. CR exhibits specific binding affinity for lipids and lipoproteins within the mycobacterial cell wall [24, 39]. The WT strain formed compact, smooth-edged colonies with moderate CR binding, whereas the *lcpAΔlytR_C* mutant produced significantly larger colonies with irregular, diffuse margins and altered staining patterns (Fig 3A, i). Quantification confirmed that the mutant exhibited a 1.5-fold increase in colony diameter compared with the WT (Fig. 3A, ii).

Biofilm formation in mycobacteria is intimately linked to cell wall composition and surface hydrophobicity, and defects in envelope integrity frequently manifest as altered biofilm architecture [40]. Therefore, we next assessed cell envelope integrity through biofilm formation assays. At the air-liquid interface, the WT developed a smooth, continuous pellicle, whereas the *lcpA*Δ*lytR_C* mutant formed fragile, discontinuous pellicle fragments with visible gaps that accumulated at the bottom of the plate (Fig. 3B, i). Crystal violet quantification revealed that total biofilm biomass after 5 days was significantly decreased by ~1.5-fold in the mutant compared with the WT (Fig. 3B, ii).

Given these observations, we hypothesized that the mutant possessed a structurally compromised cell wall, which was further confirmed by autolysis assays. Exposure to 0.01% Triton X-100 for 2 h revealed that the *lcpA*Δ*lytR_C* mutant exhibited ~2-fold heightened autolytic sensitivity compared with the WT (Fig. 3C, i). Similarly, treatment with 0.125 mg/mL lysozyme — which

hydrolyzes β-(1,4) glycosidic linkages between *N*-acetylmuramic acid (NAM) and *N*-acetylglucosamine (NAG) within PG [41, 42], for 24 h resulted in a 2.3-fold increase in sensitivity for the mutant strain, relative to the WT (Fig. 3C, ii).

To directly assess membrane permeability, we performed a Nile Red (NR) dye uptake assay. NR is a lysochrome that stains neutral lipids, and its accumulation reflects loss of envelope impermeability. At 48 h during late-log phase, the *lcpAΔlytR_C* mutant exhibited a significant 1.5-fold increase in NR fluorescence intensity compared with the WT (Fig. 3D). Collectively, these findings establish that chromosomal deletion of the LytR_C domain correlates with profound compromise in cell wall integrity and permeability barrier function.

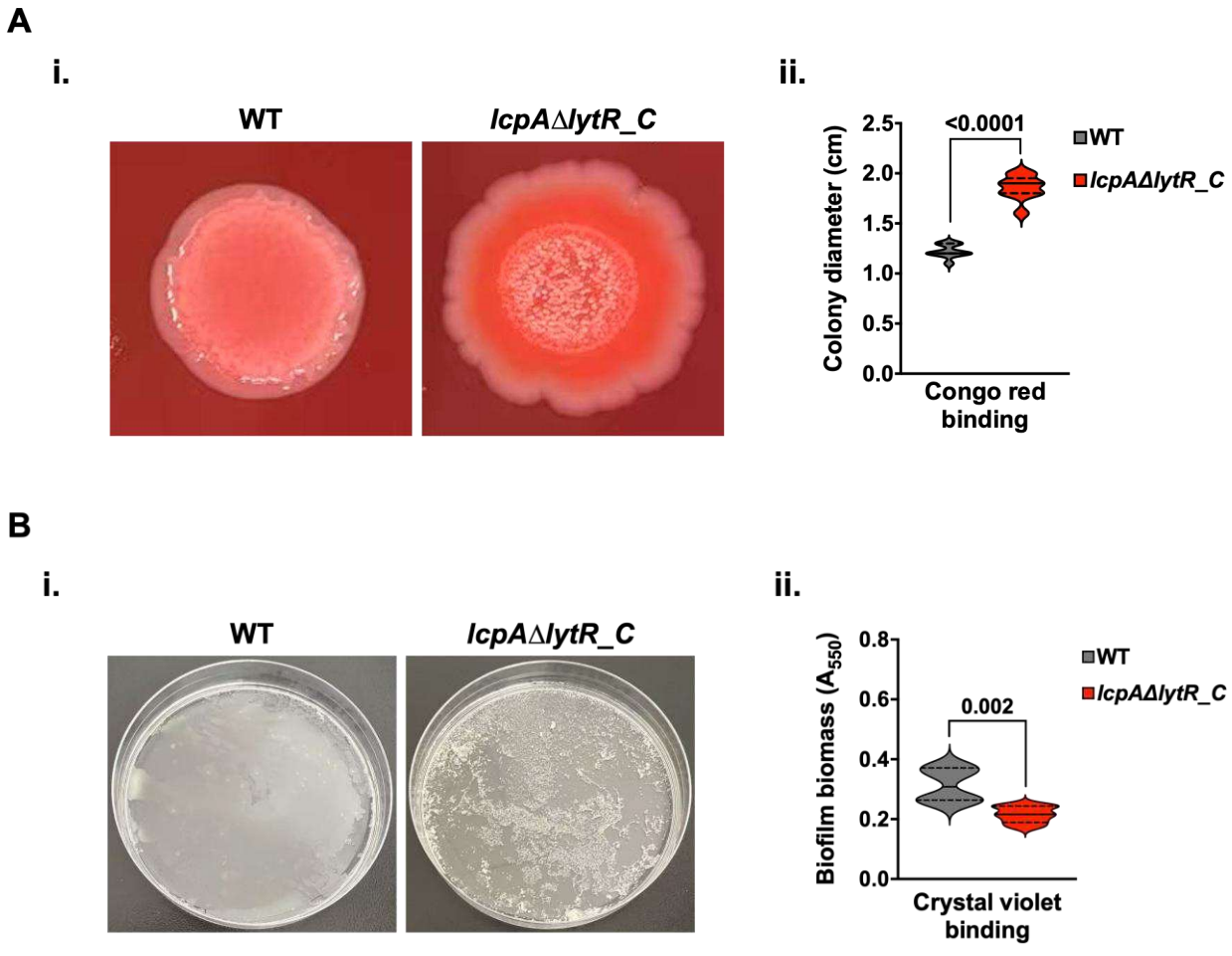

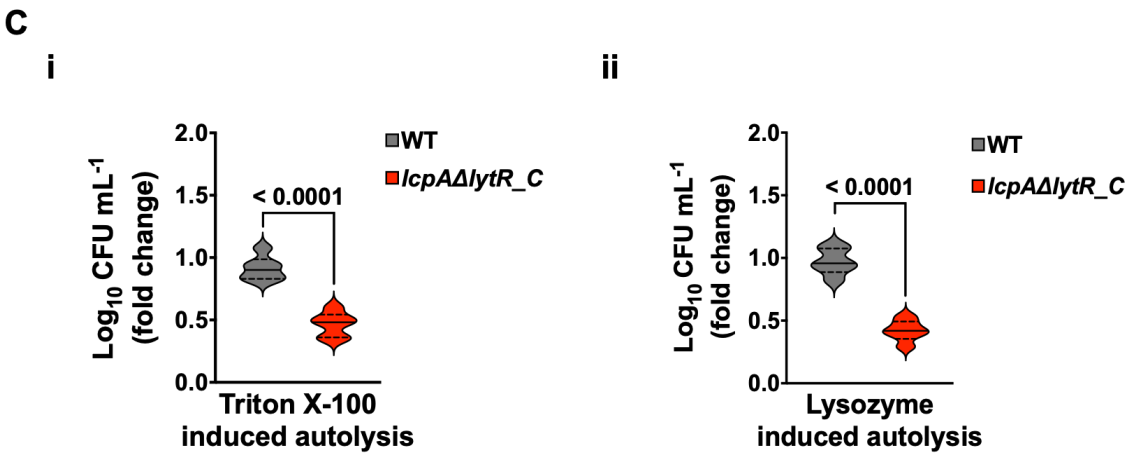

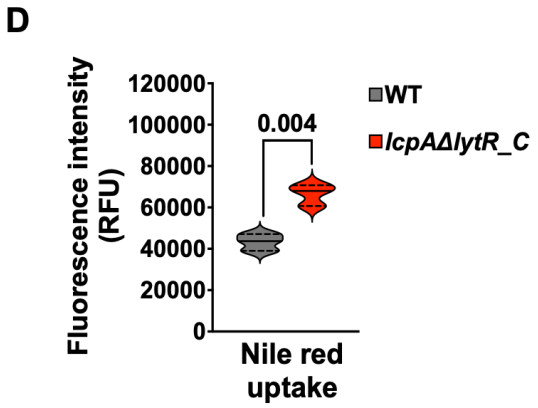

Fig 3. Impact of *lcpAΔlytR_C* mutant on cell wall permeability. A. (i) Representative colony morphologies on Congo red–containing agar. (ii) Quantification of colony diameter (cm) on Congo red plate. **B.** (i) Growth of *Msmeg* strains on air-media interface after 5-days of incubation at 37°C. (ii) Crystal violet assay for the quantification of biofilm. **C.** Autolysis assay of the *Msmeg* strains with (i) Triton X-100 and (ii) Lysozyme. **D.** Cell wall permeability assay using Nile Red, as determined at T=48h. For A-D, the represented interleaved violin plots (Median-line, Quartile-dashed) are indicative of three independent experiments each performed in triplicate. Statistical significance was determined by one-way ANOVA with Dunnett's multiple comparisons test (95% confidence level).

Surface exposure of AG and PG epitopes in the lcpAΔlytR_C mutant

The increased influx of hydrophobic dyes and heightened surface stress sensitivity led us to hypothesize that the LytR_C domain of the essential LcpA is required for maintaining the surface architecture of the mycobacterial cell envelope. To demonstrate this, whole-cell ELISA using monoclonal antibodies specific for AG (EB-A2) and PG revealed that the *lcpAΔlytR_C* mutant displayed a significant 1.2-fold increase in EB-A2 reactivity and a ~1.1-fold increase in anti-PG binding compared with the WT (Fig. 4A, i–ii). These data indicate that truncation of the LytR_C domain results in surface exposure of both AG and PG epitopes.

Given that LCP family proteins catalyze phosphodiester bond formation for ligating glycopolymers to PG [10], we postulated that increased surface exposure of the *lcpA*Δ*lytR_C* mutant might reflect altered polymer content. Consequently, we extracted cell wall material containing the mycolyl-arabinogalactan-peptidoglycan (mAGP) complex from equivalent wet cell biomass (3.2 g) across the two strains (Table 1). However, no significant differences were observed in the average yield of extracted cell wall material among these strains (Table 1). When AG-PG complexes were normalized to 200 mg of cell wall biomass, and subsequently analyzed by ELISA, the AG and PG content was comparable across these two strains (Fig. 4B, i–ii). Thus, deletion of the LytR_C domain does not substantially alter the total mass of cell wall material or the bulk AG-PG content under standard growth conditions, but rather disrupts the proper surface presentation and organization of these polymers.

Hyper susceptibility of the lcpAΔlytR_C mutant to first-line anti-TB agents

Given the compromised cell envelope of the *lcpA*Δ*lytR_C* mutant, we evaluated its susceptibility to currently prescribed anti-TB drugs. Minimum inhibitory concentrations (MICs) were determined by spot assay on CR-enriched agar (Fig. 4C, i), resazurin microtiter (REMA) assay [43]

(Fig 4C, ii and Table S3), and quantitative CFU enumeration on LB agar (Fig. 4C, iii). In the spot assay (Fig. 4C, i), the WT demonstrated robust growth in all concentrations of isoniazid (INH), ethambutol (EMB), and pyrazinamide (PZA), and only minor growth inhibition at the highest concentrations of vancomycin (VAN), streptomycin (STR), and rifampicin (RIF). Conversely, the mutant showed significantly reduced growth at substantially lower drug concentrations, with almost full growth inhibition by VAN at 50 µM and increased sensitivity to STR, RIF, EMB, and INH.

REMA confirmed these results (Fig 4C, ii and Table S3), with the mutant being substantially inhibited by VAN at lower concentrations, whereas the WT strain retained viability at higher drug levels. Quantitative CFU analysis confirmed these findings showing that after drug exposure, the mutant exhibited significantly reduced survival than the WT, with the most pronounced effect observed for VAN (4.3-fold reduction) and EMB (1.7-fold reduction), along with a modest but significant reduction after INH treatment (1.4-fold reduction). VAN is a large glycopeptide that is usually excluded from the intact mycobacterial envelope because of its hydrophilic character and molecular size [44]. In general, VAN exerted particularly strong inhibition against the mutant, consistent with a generalized loss of permeability barrier function.

Table 1. Biomass of cell wall material from different *Msmeg* strains

Strain	**Harvested wet biomass (g)**		**Extracted cell wall (mg)**	
	Exp - 1	**Exp - 2**	**Exp - 1**	**Exp – 2**
WT	3.2	3.2	236	203
lcpAΔlytR_C	3.2	3.2	227	215

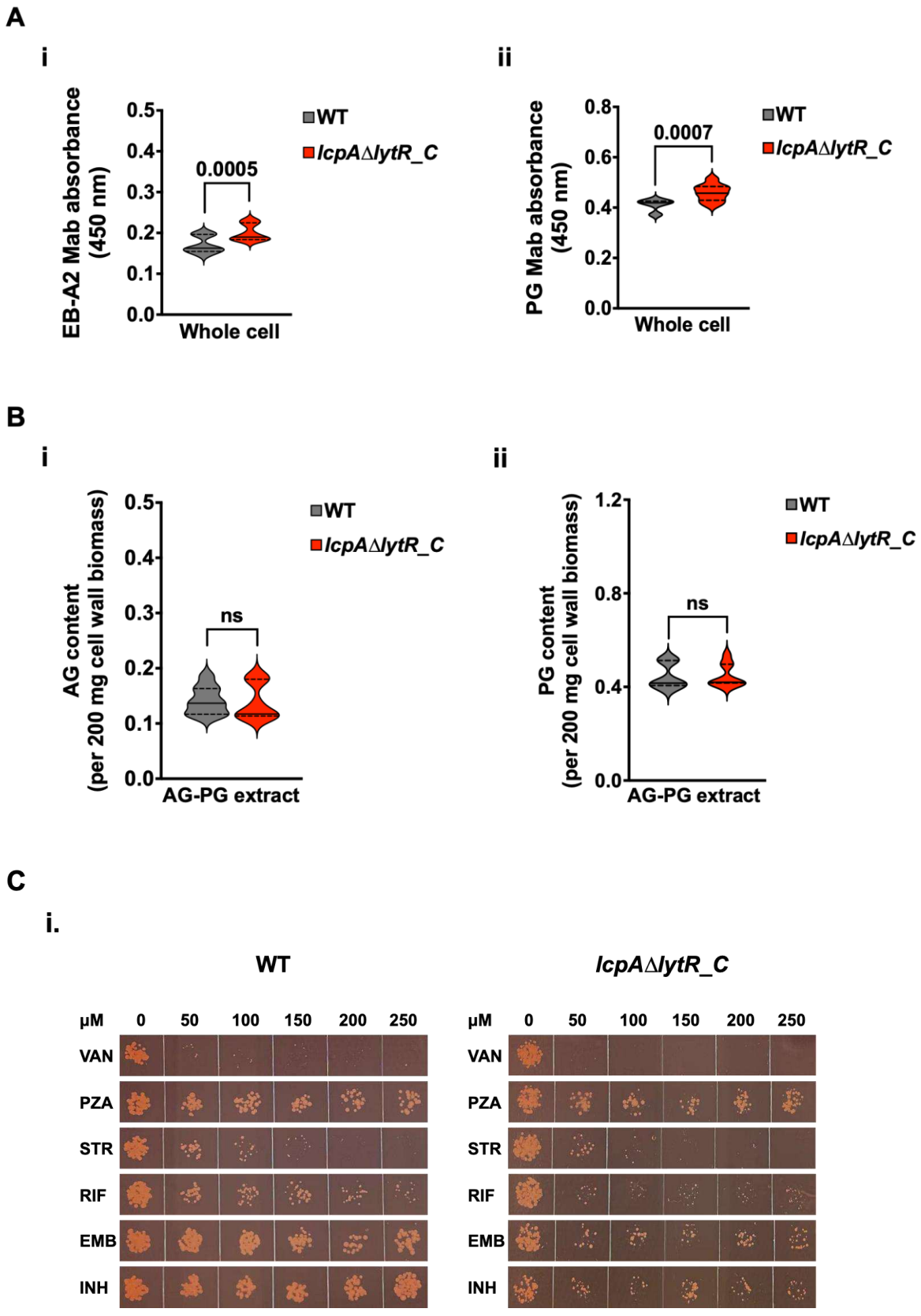
A
i
EB-A2 Mab absorbance (450 nm)
0.5
0.4
0.3
0.2
0.1
0.0
0.0005
WT
lcpAΔlytR_C
Whole cell
ii
PG Mab absorbance (450 nm)
0.8
0.6
0.4
0.2
0.0
0.0007
WT
lcpAΔlytR_C
Whole cell
B
i
AG content (per 200 mg cell wall biomass)
0.5
0.4
0.3
0.2
0.1
0.0
ns
WT
lcpAΔlytR_C
AG-PG extract
ii
PG content (per 200 mg cell wall biomass)
1.2
0.8
0.4
0.0
ns
WT
lcpAΔlytR_C
AG-PG extract
C
i.
WT
lcpAΔlytR_C
μM 0 50 100 150 200 250
VAN
PZA
STR
RIF
EMB
INH
μM 0 50 100 150 200 250
VAN
PZA
STR
RIF
EMB
INH

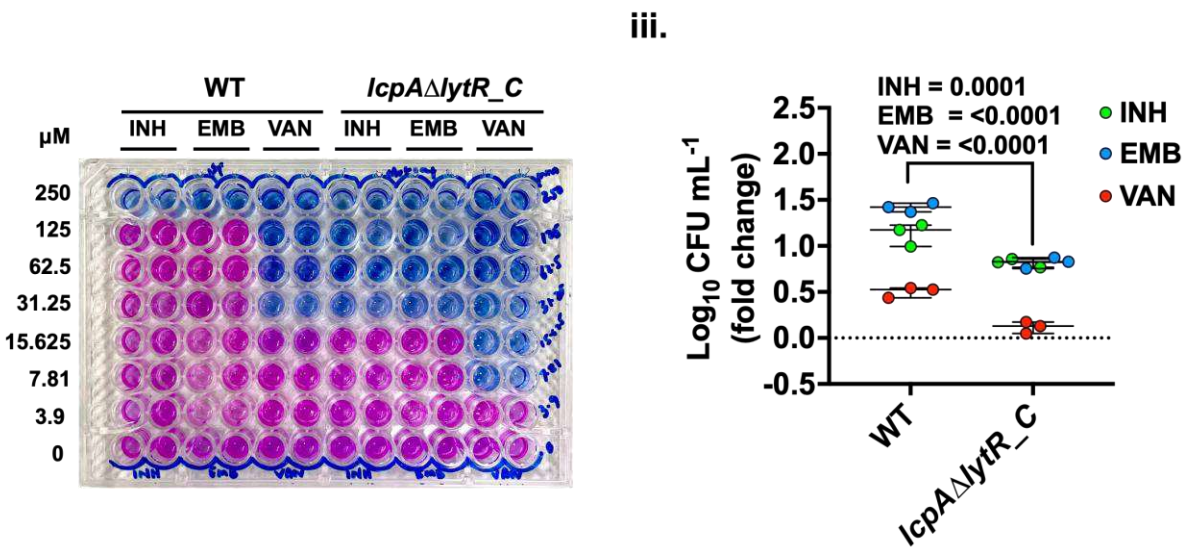

Fig 4. Drug susceptibility of *lcpAΔlytR_C* mutant. A. ELISA experiments exhibiting significant binding of (i) EB-A2 Mab and (ii) anti-PG Mab, to the whole bacterial cell of *lcpAΔlytR_C* mutant. **B.** ELISA data representing total (i) AG and (ii) PG levels detected in the AG-PG extracted cell wall matrix of *Msmeg* strains. For A and B, data is represented as interleaved violin plots (Median-line, Quartile-dashed) and are indicative of three independent experiments each performed in triplicate. **C.** (i) Congo red MIC spot assay and (ii) REMA assay of anti-TB drugs; (iii) Superimposed scatter plot displaying inhibition of *Msmeg* strains by cell wall targeting anti-TB drugs at 50 uM concentration on LB agar plates. Individual experimental values are plotted and represented as median with interquartile range, and statistical significance determined by two-way ANOVA with Tukey post-hoc analysis (95% confidence level).

Rapid clearance of lcpAΔlytR_C mutant in THP-1 macrophages

To assess whether the cell envelope defect conferred by the *lcpAΔlytR_C* mutant strain altered susceptibility to cell wall–targeting agents during intracellular infection, THP-1–derived macrophages were infected with each *Msmeg* strain and treated with INH, EMB and VAN at 10 μM concentration. Intracellular survival was monitored by CFU enumeration over 72 h.

In the absence of inhibitors, WT bacteria persisted within macrophages with a gradual decline to approximately 20–30 % survival by 72 h, whereas the *lcpAΔlytR_C* mutant exhibited significantly impaired baseline intracellular persistence, dropping to near-undetectable levels by 48 h (Fig 5). Although each drug significantly reduced WT survival over time, the bactericidal effect was markedly more pronounced in the mutant. Following VAN treatment, mutant survival approached zero by 24 h (Fig 5C), while INH and EMB similarly accelerated clearance, with the mutant reaching near-zero survival by 48 h (Fig 5, A and B). Moreover, the combination of the mutant genotype with each inhibitor resulted in significantly lower bacterial recovery than the corresponding drug-treated WT at all time points (Fig 5, A-C). Collectively, these data demonstrate that the *lcpAΔlytR_C* mutant is not only attenuated in baseline intracellular survival but also hypersusceptible to cell wall–targeting agents, with VAN — a large glycopeptide normally excluded by the intact mycobacterial envelope, exerting particularly rapid intracellular killing, consistent with a compromised cell wall permeability barrier *in vivo*.

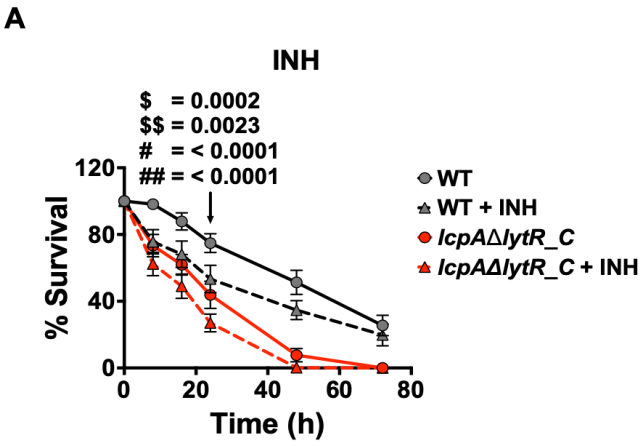

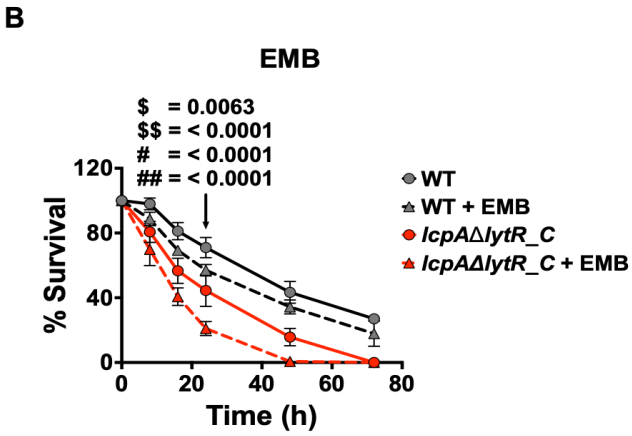

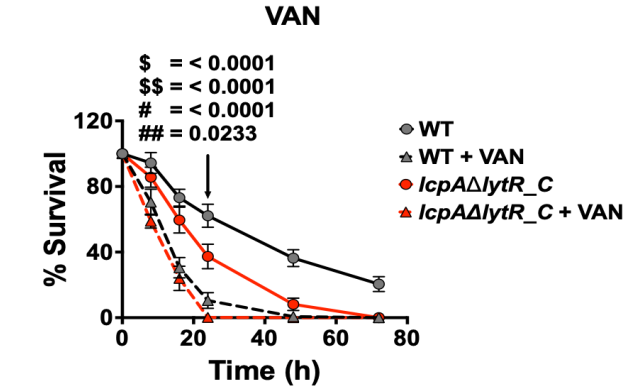

Fig 5. Intracellular survival of *Msmeg* strains in THP-1-derived macrophages following treatment with cell wall–targeting anti-TB agents. THP-1-derived macrophages were infected with WT and *lcpAΔlytR_C Msmeg* strains at MOI of 5. Infected macrophages were treated with (A) isoniazid (INH), (B) ethambutol (EMB) and (C) vancomycin (VAN) at a final concentration of 10 μM. Intracellular bacterial viability was assessed by colony-forming unit (CFU) enumeration at the indicated time points. Data represent the mean ± standard deviation (SD) from three independent experiments, each performed in duplicate. Statistical significance was determined by one-way analysis of variance (ANOVA) with Tukey's post hoc test. Symbols indicate: $ - WT vs WT+Inhibitor; $$ - *lcpAΔlytR_C* vs *lcpAΔlytR_C*+Inhibitor; # - WT vs *lcpAΔlytR_C* and ## - WT+Inhibitor vs *lcpAΔlytR_C*+Inhibitor.

DISCUSSION

The escalating global burden of multidrug-resistant *Mtb* has intensified the urgent need to identify novel therapeutic targets capable of undermining the biogenesis of the mycobacterial cell envelope, which has historically been the frontline of existing anti-TB chemotherapy [1, 3, 4]. The mycobacterial cell wall is unique among bacteria in that it is composed of PG covalently bonded to AG and esterified with mycolic acids, resulting in the mycolyl-arabinogalactan-peptidoglycan (mAGP) complex that confers remarkable structural rigidity and impermeability [45]. Central to the assembly of this macromolecular scaffold are the LytR-CpsA-Psr (LCP) family of enzymes that catalyze the transfer of lipid-linked glycopolymers onto nascent PG, thereby anchoring the mAGP complex that defines the mycobacterial cell wall [7, 8, 10, 14]. While the catalytic LCP domain has been extensively characterized by biochemical reconstitution and structural studies [7, 8, 11-14, 46], the function of the C-terminal LytR_C domain conserved across actinobacterial LcpA orthologs has remained elusive [16, 19]. Our study resolves this ambiguity by demonstrating that the LytR_C domain of the essential LcpA protein (MSMEG_1824) in *Msmeg* is dispensable for phosphotransferase activity *in vitro* yet indispensable for maintaining cell wall integrity, proper cytokinesis, and resistance to both pharmacological and host-derived stresses.

The initial observation that recombinant LcpA devoid of the LytR_C domain retained *in vitro* phosphotransferase activity comparable to the transmembrane-less LytR_C-inclusive LcpA protein (Fig 2A), was consistent with the spatial positioning of this C-terminal accessory domain distal from the catalytic pocket [18]. This finding positions the LCP domain alone as sufficient for the chemical reaction of glycopolymer ligation, aligning with the established catalytic function of this domain across Gram-positive bacteria [7, 10]. In *Mtb*, LcpA is known to be the primary phosphotransferase involved in AG-PG ligation, and synthetic lethality studies have identified

LcpA as the essential enzyme for this process in mycobacteria [14]. Our observations indicate that enzymatic competency *in vitro* is not predictive of physiological sufficiency *in vivo*, but conservation of the LCP domain across different bacterial phyla indicates its key function in cell wall assembly.

Despite the catalytic redundancy observed in biochemical assays, the chromosomal *lcpAΔlytR_C* mutant exhibited severe and unambiguous physiological defects that manifested as significantly attenuated growth, a 1.6-fold prolonged doubling time, and a striking morphological transformation characterized by pole-to-pole filamentation and failed septation, with cells averaging more than twice the length of wild-type bacilli (Fig 2, C and D). This filamentous phenotype strongly suggests a fundamental defect in the coordination of PG synthesis with septum maturation, a process intricately linked to polar elongation and divisome assembly in mycobacteria [37, 38, 47, 48]. In mycobacteria, cell division is asymmetric and tightly coupled to cell wall biosynthesis at the poles and septum, where new PG is inserted to drive elongation and cytokinesis [47, 49]. These morphological anomalies were correlated to profound biochemical and physiological indications of impaired cell membrane integrity. The mutant displayed severely defective biofilm formation, with only fragile, discontinuous cellular aggregates formed at the air-liquid interface instead of the robust pellicles observed for the WT strain (Fig 3B, i). Quantitative crystal violet staining revealed a 1.5-fold reduction in total biofilm biomass (Fig 3B, ii). In mycobacteria, biofilm development is associated with cell wall composition and surface hydrophobicity , and deficiencies in envelope integrity frequently manifest as altered biofilm architecture [40]. More importantly, the mutant exhibited increased susceptibility to both Triton X-100 (Fig 3C, i) and lysozyme (Fig 3C, ii), indicating a permeabilized and structurally compromised cell wall. Triton X-100 disrupts lipid-lipid and lipid-protein interactions in the cell envelope [50], and its enhanced bactericidal effect on

574 the mutant suggests a compromised outer membrane barrier, whereas lysozyme, which hydrolyzes
575 the β-(1,4) glycosidic linkages between *N*-acetylmuramic acid and *N*-acetylglucosamine in PG [41,
576 42], was 2.3-fold more potent against the mutant, directly implicating a defect in PG integrity or
577 accessibility. The increased influx of NR dye provided direct evidence of enhanced membrane
578 permeability (Fig 3D), as this lysochrome stains neutral lipids and its accumulation is indicative
579 of a loss of envelope impermeability [51].
580 Concordantly, whole-cell ELISA assays performed using Mabs directed against AG and PG
581 revealed exposed cell wall epitopes on the surface of the mutant, in agreement with a disorganized
582 or thinner outer envelope (Fig 4A). Notably, when equivalent wet cell biomass was processed for
583 cell wall extraction, the total yield of cell wall material and the bulk AG-PG content were
584 comparable across both WT and the mutant strains (Table 1; Fig 4B), indicating that the LytR_C
585 domain does not influence the overall synthetic capacity of the cell wall machinery but rather
586 ensures the proper spatial organization and surface presentation of these polymers.
587 The compromised envelope translated directly into profound therapeutic vulnerability. The mutant
588 showed significantly reduced MICs and markedly lower CFUs when challenged with INH, EMB,
589 and VAN (Fig 4C), agents that target distinct biosynthetic pathways within the mycobacterial cell
590 wall [3, 4]. INH inhibits the enoyl-ACP reductase InhA in the type II fatty acid synthase (FAS-II)
591 pathway of mycolic acid biosynthesis [52-54], targets the arabinosyltransferases EmbA and EmbB,
592 which catalyze the polymerization and branching of arabinose residues in AG [55, 56], and VAN
593 interferes with PG cross-linking by binding to the D-Ala-D-Ala terminus of lipid II, thereby
594 inhibiting transglycosylase and transpeptidase activities [2, 57, 58]. The hypersensitivity of
595 *lcpAΔlytR_C* mutant to all the three agents suggests a generalized compromise of cell wall
596 homeostasis rather than a pathway-specific defect, likely multifactorial in origin: the compromised

barrier function may facilitate enhanced drug penetration, while the general disorganization of the envelope could impair efflux pump activity or alter the local redox environment necessary for pro-drug activation [3, 4, 44]. The particularly potent activity of VAN — a large glycopeptide normally excluded by the intact mycobacterial envelope, against the mutant underscores the severity of the permeability defect. The use of Congo Red-enriched agar in the susceptibility assays further emphasised the mutant's fundamentally altered surface architecture, as Congo Red binds lipids and lipoproteins in the mycobacterial cell wall, and its uptake is modulated by envelope integrity [24, 39]. These findings are significant, given that majority of the present day anti-TB regimens target cell wall biosynthesis [3, 4], and imply that inhibitors targeted against the LytR_C domain could serve as potent sensitizers capable of lowering effective doses of existing drugs and potentially shortening treatment duration.

Beyond *in vitro* susceptibility, the biological relevance of the LytR_C domain was starkly demonstrated by the mutant's inability to survive within host macrophages. Moreover, the *lcpAΔlytR_C* strain was rapidly cleared from THP-1-derived macrophages even in the absence of exogenous antibiotics, with bacterial numbers reaching zero by 72 hours post-infection (Fig 5). When macrophages were treated with sub-inhibitory concentrations of cell wall-targeting drugs, bacterial survival was further reduced, with VAN reducing the mutant’s survival to near-zero by 24 hours and INH and EMB accelerated clearance by 48 hours. This rapid clearance likely reflects a combination of increased susceptibility to host-derived oxidative and nitrosative stresses, enhanced recognition by pattern recognition receptors through exposed cell wall components, and impaired ability to withstand the acidic, nutrient-limited environment of the phagolysosome. Although *Msmeg* is an avirulent surrogate, the strict orthology between MSMEG_1824 and Rv3267 in *Mtb* significantly supports the hypothesis that the LytR_C domain performs a conserved,

620 critical function in pathogenic mycobacteria. In *Mtb*, the LCP protein CpsA (Rv3484) was
621 demonstrated to protect the bacillus against NADPH oxidase-mediated death and LC3-associated
622 phagocytosis in macrophages [59], emphasising the wider role of the LCP family for intracellular
623 survival [10]. If the LytR_C domain of LcpA performs an analogous scaffolding or protective
624 function in *Mtb*, its disruption could compromise the pathogen's ability to persist within host
625 macrophages, a prerequisite for latent infection and disease progression.
626 The viability of *lcpAΔlytR_C* mutant despite such severe morphological and physiological defects
627 suggests that the remaining LytR_C-containing Lcp proteins (LcpB and LcpC) and/or LytR_C
628 domain-only proteins can partially compensate for the lost function, providing basal levels of AG-
629 PG ligation that sustain essential envelope synthesis. Nevertheless, the profound elongation,
630 division failure and cell wall fragility observed, suggest that this compensatory activity is
631 insufficient to preserve WT envelope architecture and resilience. Collectively, our data suggest a
632 hypothesis in which the LytR_C domain functions as a structural or regulatory scaffold that ensures
633 appropriate assembly, stability or spatial localization of the cell wall ligase complex. In this
634 hypothesis, the LCP domain catalyzes the crucial chemical reaction of AG-PG ligation [7, 14], while
635 the LytR_C domain organizes the enzyme into functional oligomers or tethers it to the divisome
636 or elongasome, thereby coordinating PG synthesis with cytokinesis. This is in line with findings
637 in *C. glutamicum*, where LcpA uniquely forms dimers and tetramers, a feature thought to be
638 dependent on the LytR_C domain, and where both domains were found to be essential for full
639 protein function [16]. If oligomerization is indeed mediated by the LytR_C domain, its deletion
640 would disrupt the higher-order protein complexes necessary for efficient substrate channeling and
641 coordinated cell wall assembly, leading to the pleiotropic abnormalities we observed. The
642 evolutionary conservation of this domain across actinobacteria (Fig 1, A-B), including six invariant

residues identified in our phylogenetic analysis (Fig 1, C), further indicates its functional relevance despite being structurally separable from the catalytic core. The distinct evolutionary clustering of the LytR_C domains of LcpA, LcpB, and LcpC orthologs further suggests that this auxiliary domain may have evolved to fulfil the specific physiological demands of each paralog. In *Streptococcus pneumoniae*, the LytR protein is required for normal septum formation [60], and in *Staphylococcus aureus*, LCP enzymes link capsular polysaccharide to PG [12] through mechanisms that may similarly rely on accessory domains for proper localization. Thus, the necessity of LytR_C domain in maintaining cell shape and division may represent a conserved feature in Gram-positive bacteria with complex cell envelopes.

Together, our results reveal a previously unrecognized role of the LytR_C domain of the essential LcpA protein in preserving the mycobacterial cell envelope integrity. By segregating catalytic activity from structural scaffolding that could distort cell wall homeostasis, sensitize the pathogen to existing therapies, and impair intracellular survival, this auxillary domain emerges as a unique and intriguing target for the development of novel anti-TB drugs. Given the strict conservation of the LytR_C domain across actinobacteria, including *Mtb*, our findings provide the groundwork for future translational studies focused on leveraging this domain as a vulnerability in one of the world's most formidable bacterial pathogens.

CONCLUSION

The LytR_C domain of essential LcpA is separable from the catalytic LCP domain. It is not required for *in vitro* ligase activity but is critical for cell-envelope integrity, normal cell division, drug tolerance and intracellular persistence.

LIMITATIONS OF THE STUDY

Our experiments were conducted in *Msmeg*, which, despite being the most robust genetically tractable model for mycobacterial cell envelope biology, differs in growth rate, pathogenicity, and cell wall lipid composition from *Mtb*. Confirmation of these findings in *Mtb* or in an animal model of infection is therefore essential to validate the LytR_C domain as a therapeutic target in the pathogen itself. Furthermore, our *in vitro* kinase assay utilized truncated recombinant proteins lacking the transmembrane anchor and a synthetic substrate analog (GPP), which may not fully recapitulate the complexity of native lipid-linked substrates, membrane-associated assembly and potential allosteric regulation in the physiological context of the intact cell envelope. The precise molecular mechanism by which the LytR_C domain influences PG content, whether through direct protein-protein interactions, oligomerization, membrane microdomain organization, or modulation of substrate access, remains to be elucidated. Structural studies, such as cryo-electron microscopy of full-length and LytR_C-deleted LcpA in a membrane context, combined with native mass spectrometry, cross-linking mass spectrometry and co-immunoprecipitation experiments, will be crucial to define the mechanistic basis of this domain's scaffolding function. Finally, the development of small-molecule inhibitors or peptidomimetics targeting the conserved residues within the LytR_C domain, followed by *in vitro* and *in vivo* efficacy testing, will be necessary to validate its druggability and provide lead compounds for anti-TB drug discovery.

LIST OF ABBREVIATIONS

TB, Tuberculosis

***Mtb*,** *Mycobacterium tuberculosis*

LCP, LytR-CpsA-Psr

AG, Arabinogalactan

PG, Peptidoglycan

***Msmeg*,** *Mycolicibacterium smegmatis*

PCR, Polymerase chain reaction

RT-qPCR, Reverse transcriptase quantitative polymerase chain reaction

PBS, Phosphate-buffered saline

OD, Optical density

BSA, Bovine serum albumin

SEM, Scanning electron microscopy

CFU, Colony-forming unit

CR, Congo Red

NR, Nile Red

***E. coli*,** *Escherichia coli*

INH, Isoniazid

EMB, Ethambutol

STR, Streptomycin

RIF, Rifampicin

VAN, Vancomycin

PZA, Pyrazinamide

ELISA, Enzyme-linked immunosorbent assay

FAS-II, Fatty acid synthase II

GPP, Geranyl pyrophosphate

HRP, Horseradish peroxidase

MIC, Minimum inhibitory concentration

TM, Transmembrane

IPTG, Isopropyl β-D-1-thiogalactopyranoside

LB, Luria-Bertani

ATP, Adenosine triphosphate

mAGP, Mycolyl-arabinogalactan-peptidoglycan

MOI, Multiplicity of infection

NAG, N-acetylglucosamine

NAM, N-acetylmuramic acid

PMA, Phorbol 12-myristate 13-acetate

REMA, Resazurin microtiter assay

WT, Wild type

DECLARATIONS

Ethics approval and consent to participate

Not applicable

Consent for publication

Not applicable

Clinical trial number

Not applicable

Availability of data and materials

The nucleotide sequences supporting our attempt to generate the complement construct with *rfbD* promoter region is available in the NCBI Genbank repository with accession numbers: QB321687, QB321688, QB321689 and QB321690. These dataset(s) represent the successful cloning of *rfbD* sequences only, in two different recombinant pSMT3 complement constructs.

Competing Interests

The authors declare that they have no competing interests.

Funding

This project was financially supported by Jiangsu Province Doctoral Fund in Entrepreneurship and Innovation (JSSCBS20222474) and Taizhou 113 talent fund. The funders had no role in study design, data collection and analysis, decision to publish, or preparation of the manuscript.

Authors' contributions

A.S. was involved in conception and design of the study. A.S. and L.Z. have acquired experimental data. A.S. has analyzed and (or) interpreted the data. A.S., B.T., D.R.C., J.M.L. and Y.Y. have written or reviewed the manuscript.

Acknowledgements

We thank Yomiyu Mitiku Wakjira for his technical assistance in generating preliminary experimental data. We are further grateful to Dr. Dhiraj Kumar (ICGEB, New Delhi) for his proficient advice in improving the manuscript.

REFERENCES

1. WHO Global Tuberculosis Report. *World Health Organization* (2025).
2. Zhang, Y., Wu, R., Sun, M., Li, X., Fang, R., Xing, J., Li, Z., Wen, Y. & Song, N. Progress of anti-tuberculosis drug targets and novel therapeutic strategies. *Front Microbiol* **16**, 1637254 (2025).
3. Jackson, M., McNeil, M.R. & Brennan, P.J. Progress in targeting cell envelope biogenesis in *Mycobacterium tuberculosis*. *Future Microbiol* **8**, 855-875 (2013).
4. Xu, X., Dong, B., Peng, L., Gao, C., He, Z., Wang, C. & Zeng, J. Anti-tuberculosis drug development via targeting the cell envelope of *Mycobacterium tuberculosis*. *Front Microbiol* **13**, 1056608 (2022).
5. Warth, A.D. & Strominger, J.L. Structure of the peptidoglycan from vegetative cell walls of *Bacillus subtilis*. *Biochemistry* **10**, 4349-4358 (1971).
6. Weidel, W. & Pelzer, H. Bagshaped macromolecules-a new outlook on bacterial cell walls. *Adv Enzymol Relat Subj Biochem* **26**, 193-232 (1964).
7. Schaefer, K., Matano, L.M., Qiao, Y., Kahne, D. & Walker, S. *In vitro* reconstitution demonstrates the cell wall ligase activity of LCP proteins. *Nat Chem Biol* **13**, 396-401 (2017).
8. Kawai, Y., Marles-Wright, J., Cleverley, R.M., Emmins, R., Ishikawa, S., Kuwano, M., Heinz, N., Bui, N.K., Hoyland, C.N., Ogasawara, N., Lewis, R.J., Vollmer, W., Daniel, R.A. & Errington, J. A widespread family of bacterial cell wall assembly proteins. *EMBO J* **30**, 4931-4941 (2011).
9. Hubscher, J., Luthy, L., Berger-Bachi, B. & Stutzmann Meier, P. Phylogenetic distribution and membrane topology of the LytR-CpsA-Psr protein family. *BMC Genomics* **9**, 617 (2008).
10. Stefanovic, C., Hager, F.F. & Schaffer, C. LytR-CpsA-Psr glycopolymer transferases: essential bricks in Gram-Positive bacterial cell wall assembly. *Int J Mol Sci* **22** (2021).
11. Schaefer, K., Owens, T.W., Kahne, D. & Walker, S. Substrate preferences establish the order of cell wall assembly in *Staphylococcus aureus*. *J Am Chem Soc* **140**, 2442-2445 (2018).
12. Chan, Y.G., Kim, H.K., Schneewind, O. & Missiakas, D. The capsular polysaccharide of *Staphylococcus aureus* is attached to peptidoglycan by the LytR-CpsA-Psr (LCP) family of enzymes. *J Biol Chem* **289**, 15680-15690 (2014).
13. Eberhardt, A., Hoyland, C.N., Vollmer, D., Bisle, S., Cleverley, R.M., Johnsborg, O., Havarstein, L.S., Lewis, R.J. & Vollmer, W. Attachment of capsular polysaccharide to the cell wall in *Streptococcus pneumoniae*. *Microb Drug Resist* **18**, 240-255 (2012).
14. Harrison, J., Lloyd, G., Joe, M., Lowary, T.L., Reynolds, E., Walters-Morgan, H., Bhatt, A., Lovering, A., Besra, G.S. & Alderwick, L.J. Lcp1 is a phosphotransferase responsible for ligating arabinogalactan to peptidoglycan in *Mycobacterium tuberculosis*. *mBio* **7** (2016).

15. Sigle, S., Steblau, N., Wohlleben, W. & Muth, G. Polydiglycosylphosphate transferase PdtA (SCO2578) of *Streptomyces coelicolor* A3(2) is crucial for proper sporulation and apical tip extension under stress conditions. *Appl Environ Microbiol* **82**, 5661-5672 (2016).
16. Baumgart, M., Schubert, K., Bramkamp, M. & Frunzke, J. Impact of LytR-CpsA-Psr proteins on cell wall biosynthesis in *Corynebacterium glutamicum*. *J Bacteriol* **198**, 3045-3059 (2016).
17. Wu, C., Huang, I.H., Chang, C., Reardon-Robinson, M.E., Das, A. & Ton-That, H. Lethality of sortase depletion in *Actinomyces oris* caused by excessive membrane accumulation of a surface glycoprotein. *Mol Microbiol* **94**, 1227-1241 (2014).
18. Sahu, A., Xie, Z., Cheng, H.J., Omoboyowa, D.A., Zhang, L., Zhai, X.C., Bitter, W., Ruiz-Carrillo, D., Tefsen, B., Li, J.M. & Yang, Y. Impairment of two non-essential LytR-cpsA-psr (Lcp) cell wall ligases decelerate cell wall assembly in *Mycolicibacterium smegmatis*. *BMC Microbiol* **26** (2026).
19. Bhowmick, S., Viveros, R.P., Latoscha, A., Commichau, F.M., Wrede, C., Al-Bassam, M.M. & Tschowri, N. Cell shape and division septa positioning in filamentous *Streptomyces* require a functional cell wall glycopolymer ligase CglA. *mBio* **15**, e0149224 (2024).
20. Nuovo, G., Tili, E., Suster, D., Matys, E., Hupp, L. & Magro, C. Strong homology between SARS-CoV-2 envelope protein and a *Mycobacterium* sp. antigen allows rapid diagnosis of mycobacterial infections and may provide specific anti-SARS-CoV-2 immunity via the BCG vaccine. *Ann Diagn Pathol* **48**, 151600 (2020).
21. Ballister, E.R., Samanovic, M.I. & Darwin, K.H. *Mycobacterium tuberculosis* Rv2700 contributes to cell envelope integrity and virulence. *J Bacteriol* **201**, e00228-00219 (2019).
22. Ofer, N., Wishkautzan, M., Meijler, M., Wang, Y., Speer, A., Niederweis, M. & Gur, E. Ectoine biosynthesis in *Mycobacterium smegmatis*. *Appl Environ Microbiol* **78**, 7483-7486 (2012).
23. Cui, G., Wang, J., Qi, X. & Su, J. Transcription elongation factor GreA plays a key role in cellular invasion and virulence of *Francisella tularensis* subsp. *novicida*. *Sci Rep* **8**, 6895 (2018).
24. Cangelosi, G.A., Palermo, C.O., Laurent, J.P., Hamlin, A.M. & Brabant, W.H. Colony morphotypes on Congo red agar segregate along species and drug susceptibility lines in the *Mycobacterium avium-intracellulare* complex. *Microbiology (Reading)* **145 (Pt 6)**, 1317-1324 (1999).
25. Bharati, B.K., Sharma, I.M., Kasetty, S., Kumar, M., Mukherjee, R. & Chatterji, D. A full-length bifunctional protein involved in c-di-GMP turnover is required for long-term survival under nutrient starvation in *Mycobacterium smegmatis*. *Microbiology* **158**, 1415-1427 (2012).
26. Zanfardino, A., Migliardi, A., D'Alonzo, D., Lombardi, A., Varcamonti, M. & Cordone, A. Inactivation of *MSMEG_0412* gene drastically affects surface related properties of *Mycobacterium smegmatis*. *BMC Microbiol* **16**, 267 (2016).

27. Ojha, A.K., Baughn, A.D., Sambandan, D., Hsu, T., Trivelli, X., Guerardel, Y., Alahari, A., Kremer, L., Jacobs, W.R., Jr. & Hatfull, G.F. Growth of *Mycobacterium tuberculosis* biofilms containing free mycolic acids and harbouring drug-tolerant bacteria. *Mol Microbiol* **69**, 164-174 (2008).
28. Yan, S., Xu, M., Wang, R., Li, Q., Yu, Z. & Xie, J. Overexpression of Rv2788 increases mycobacterium stresses survival. *Microbiol Res* **195**, 51-59 (2017).
29. Agrawal, P., Miryala, S. & Varshney, U. Use of *Mycobacterium smegmatis* deficient in ADP-ribosyltransferase as surrogate for *Mycobacterium tuberculosis* in drug testing and mutation analysis. *PLoS One* **10**, e0122076 (2015).
30. Tamura, K., Stecher, G. & Kumar, S. MEGA11: Molecular Evolutionary Genetics Analysis Version 11. *Mol Biol Evol* **38**, 3022-3027 (2021).
31. Saitou, N. & Nei, M. The neighbor-joining method: a new method for reconstructing phylogenetic trees. *Mol Biol Evol* **4**, 406-425 (1987).
32. Nei, M. & Kumar, S. Molecular evolution and phylogenetics. *Oxford University Press, New York* (2000).
33. Felsenstein, J. Confidence limits on phylogenies: an approach using the bootstrap. *Evolution* **39**, 783-791 (1985).
34. Stecher, G., Tamura, K. & Kumar, S. Molecular Evolutionary Genetics Analysis (MEGA) for macOS. *Mol Biol Evol* **37**, 1237-1239 (2020).
35. Robert, X., Guillon, C. & Gouet, P. FoldScript: a web server for the efficient analysis of AI-generated 3D protein models. *Nucleic Acids Res* **53**, W277-W282 (2025).
36. Dahl, J.L., Arora, K., Boshoff, H.I., Whiteford, D.C., Pacheco, S.A., Walsh, O.J., Lau-Bonilla, D., Davis, W.B. & Garza, A.G. The *relA* homolog of *Mycobacterium smegmatis* affects cell appearance, viability, and gene expression. *J Bacteriol* **187**, 2439-2447 (2005).
37. Aldridge, B.B., Fernandez-Suarez, M., Heller, D., Ambravaneswaran, V., Irimia, D., Toner, M. & Fortune, S.M. Asymmetry and aging of mycobacterial cells lead to variable growth and antibiotic susceptibility. *Science* **335**, 100-104 (2012).
38. Santi, I., Dhar, N., Bousbaine, D., Wakamoto, Y. & McKinney, J.D. Single-cell dynamics of the chromosome replication and cell division cycles in mycobacteria. *Nat Commun* **4**, 2470 (2013).
39. Etienne, G., Villeneuve, C., Billman-Jacobe, H., Astarie-Dequeker, C., Dupont, M.A. & Daffe, M. The impact of the absence of glycopeptidolipids on the ultrastructure, cell surface and cell wall properties, and phagocytosis of *Mycobacterium smegmatis*. *Microbiology* **148**, 3089-3100 (2002).
40. Singh, P., Rao, R.N., Reddy, J.R., Prasad, R.B., Kotturu, S.K., Ghosh, S. & Mukhopadhyay, S. PE11, a PE/PPE family protein of *Mycobacterium tuberculosis* is involved in cell wall remodeling and virulence. *Sci Rep* **6**, 21624 (2016).

41. Nawaz, N., Wen, S., Wang, F., Nawaz, S., Raza, J., Iftikhar, M. & Usman, M. Lysozyme and its application as antibacterial agent in food industry. *Molecules* **27** (2022).
42. Tanaka, I., Nishinomiya, R., Goto, R., Shimazaki, S. & Chatake, T. Recent structural insights into the mechanism of lysozyme hydrolysis. *Acta Crystallogr D Struct Biol* **77**, 288-292 (2021).
43. Palomino, J.C., Martin, A., Camacho, M., Guerra, H., Swings, J. & Portaels, F. Resazurin microtiter assay plate: simple and inexpensive method for detection of drug resistance in *Mycobacterium tuberculosis*. *Antimicrob Agents Chemother* **46**, 2720-2722 (2002).
44. Soetaert, K., Rens, C., Wang, X.M., De Bruyn, J., Laneelle, M.A., Laval, F., Lemassu, A., Daffe, M., Bifani, P., Fontaine, V. & Lefevre, P. Increased vancomycin susceptibility in mycobacteria: a new approach to identify synergistic activity against multidrug-resistant mycobacteria. *Antimicrob Agents Chemother* **59**, 5057-5060 (2015).
45. Alderwick, L.J., Harrison, J., Lloyd, G.S. & Birch, H.L. The mycobacterial cell wall—peptidoglycan and arabinogalactan. *Cold Spring Harb Perspect Med* **5**, a021113 (2015).
46. Grzegorzewicz, A.E., de Sousa-d'Auria, C., McNeil, M.R., Huc-Claustre, E., Jones, V., Petit, C., Angala, S.K., Zemanova, J., Wang, Q., Belardinelli, J.M., Gao, Q., Ishizaki, Y., Mikusova, K., Brennan, P.J., Ronning, D.R., Chami, M., Houssin, C. & Jackson, M. Assembling of the *Mycobacterium tuberculosis* cell wall core. *J Biol Chem* **291**, 18867-18879 (2016).
47. Kieser, K.J. & Rubin, E.J. How sisters grow apart: mycobacterial growth and division. *Nat Rev Microbiol* **12**, 550-562 (2014).
48. Adams, D.W. & Errington, J. Bacterial cell division: assembly, maintenance and disassembly of the Z ring. *Nat Rev Microbiol* **7**, 642-653 (2009).
49. Meniche, X., Otten, R., Siegrist, M.S., Baer, C.E., Murphy, K.C., Bertozzi, C.R. & Sassetti, C.M. Subpolar addition of new cell wall is directed by DivIVA in mycobacteria. *Proc Natl Acad Sci U S A* **111**, E3243-3251 (2014).
50. Seddon, A.M., Curnow, P. & Booth, P.J. Membrane proteins, lipids and detergents: not just a soap opera. *Biochim Biophys Acta* **1666**, 105-117 (2004).
51. Greenspan, P., Mayer, E.P. & Fowler, S.D. Nile red: a selective fluorescent stain for intracellular lipid droplets. *J Cell Biol* **100**, 965-973 (1985).
52. Banerjee, A., Dubnau, E., Quemard, A., Balasubramanian, V., Um, K.S., Wilson, T., Collins, D., de Lisle, G. & Jacobs, W.R., Jr. *inhA*, a gene encoding a target for isoniazid and ethionamide in *Mycobacterium tuberculosis*. *Science* **263**, 227-230 (1994).
53. Dessen, A., Quemard, A., Blanchard, J.S., Jacobs, W.R., Jr. & Sacchettini, J.C. Crystal structure and function of the isoniazid target of *Mycobacterium tuberculosis*. *Science* **267**, 1638-1641 (1995).

54. Quemard, A., Sacchettini, J.C., Dessen, A., Vilcheze, C., Bittman, R., Jacobs, W.R., Jr. & Blanchard, J.S. Enzymatic characterization of the target for isoniazid in *Mycobacterium tuberculosis*. *Biochemistry* **34**, 8235-8241 (1995).
55. Belanger, A.E., Besra, G.S., Ford, M.E., Mikusova, K., Belisle, J.T., Brennan, P.J. & Inamine, J.M. The *embAB* genes of *Mycobacterium avium* encode an arabinosyl transferase involved in cell wall arabinan biosynthesis that is the target for the antimycobacterial drug ethambutol. *Proc Natl Acad Sci U S A* **93**, 11919-11924 (1996).
56. Amin, A.G., Goude, R., Shi, L., Zhang, J., Chatterjee, D. & Parish, T. EmbA is an essential arabinosyltransferase in *Mycobacterium tuberculosis*. *Microbiology (Reading)* **154**, 240-248 (2008).
57. Reynolds, P.E. Structure, biochemistry and mechanism of action of glycopeptide antibiotics. *Eur J Clin Microbiol Infect Dis* **8**, 943-950 (1989).
58. Kim, S.J., Matsuoka, S., Patti, G.J. & Schaefer, J. Vancomycin derivative with damaged D-Ala-D-Ala binding cleft binds to cross-linked peptidoglycan in the cell wall of *Staphylococcus aureus*. *Biochemistry* **47**, 3822-3831 (2008).
59. Koster, S., Upadhyay, S., Chandra, P., Papavinasasundaram, K., Yang, G., Hassan, A., Grigsby, S.J., Mittal, E., Park, H.S., Jones, V., Hsu, F.F., Jackson, M., Sassetti, C.M. & Philips, J.A. *Mycobacterium tuberculosis* is protected from NADPH oxidase and LC3-associated phagocytosis by the LCP protein CpsA. *Proc Natl Acad Sci U S A* **114**, E8711-E8720 (2017).
60. Johnsborg, O. & Havarstein, L.S. Pneumococcal LytR, a protein from the LytR-CpsA-Psr family, is essential for normal septum formation in *Streptococcus pneumoniae*. *J Bacteriol* **191**, 5859-5864 (2009).

Supplementary Files

This is a list of supplementary files associated with this preprint. Click to download.

- 20261114RoleofLcpALytRCdomaininMycolicibacteriumsmegmatisBMCMicrobiolSupplementaryfile.docx